

of approximately 3 kb of homology: ~2 kb 5' arm and ~1 kb 3' arm. The targeting vector was introduced into embryonic stem cells derived from the 129/OlaHsd mouse strain. Targeting events were first identified by PCR on the 5' end with a GPR21 specific oligonucleotide ATG TGC TAG GGA CTG GGA GAG TAG G and three neo-specific oligonucleotides. The three PCR reactions gave the expected size of 3025, 3035 and 3600 bp respectively. PCR was used to confirm the targeting events on the 3' end of the insertion. A GPR21 specific oligonucleotide CCG TGC TCA CAT TAC TCA TCC TAT GG and three neo-specific nucleotides were used in three separate PCR reactions and resulted in three bands of expected sizes: 2300, 2250 and 1550 bp respectively. Correct homologous recombination was further confirmed by Southern blot analysis of ES cells genomic DNA after digestion with *HindIII*, using a probe located outside of the arms of homology. As expected from the insertion of the *HindIII* site in the LacZ/Neo cassette, the targeted clone gave two bands while the untransfected clone showed one band only.

Targeted ES cell clones were injected into host blastocysts and resulting chimeric mice were bred to C57BL/6J mice to generate F1 heterozygotes. F1 heterozygotes are backcrossed to C57BL/6J mice for one generation. The resulting N1F1 heterozygous males and females were backcrossed to congenicity to C57BL/6J mice as confirmed by microsatellite markers (Charles River Laboratories). GPR21 homozygous mutant mice were obtained from heterozygous mating according to a standard Mendelian transmission ratio. They appeared normal and reproduced normally.

Genotyping was performed by PCR using the following three oligonucleotides: GPR21-5': ATA CAG AGG CGT AGT CTC CAG GGA G, neo-specific: GGG CCA GCT CAT TCC TCC CAC TCA T, GPR21-3': AGT GAC AGT AGC TGC TCC TGA GAA C. The WT band had an expected size of 526 bp. The mutant band had an expected size of 319 bp.

Mice were housed in a specific-pathogen free animal facility with standard 12:12 dark-light cycle, with access to standard chow (Harlan Teklad Global Diets #2020) and water ad libitum. For

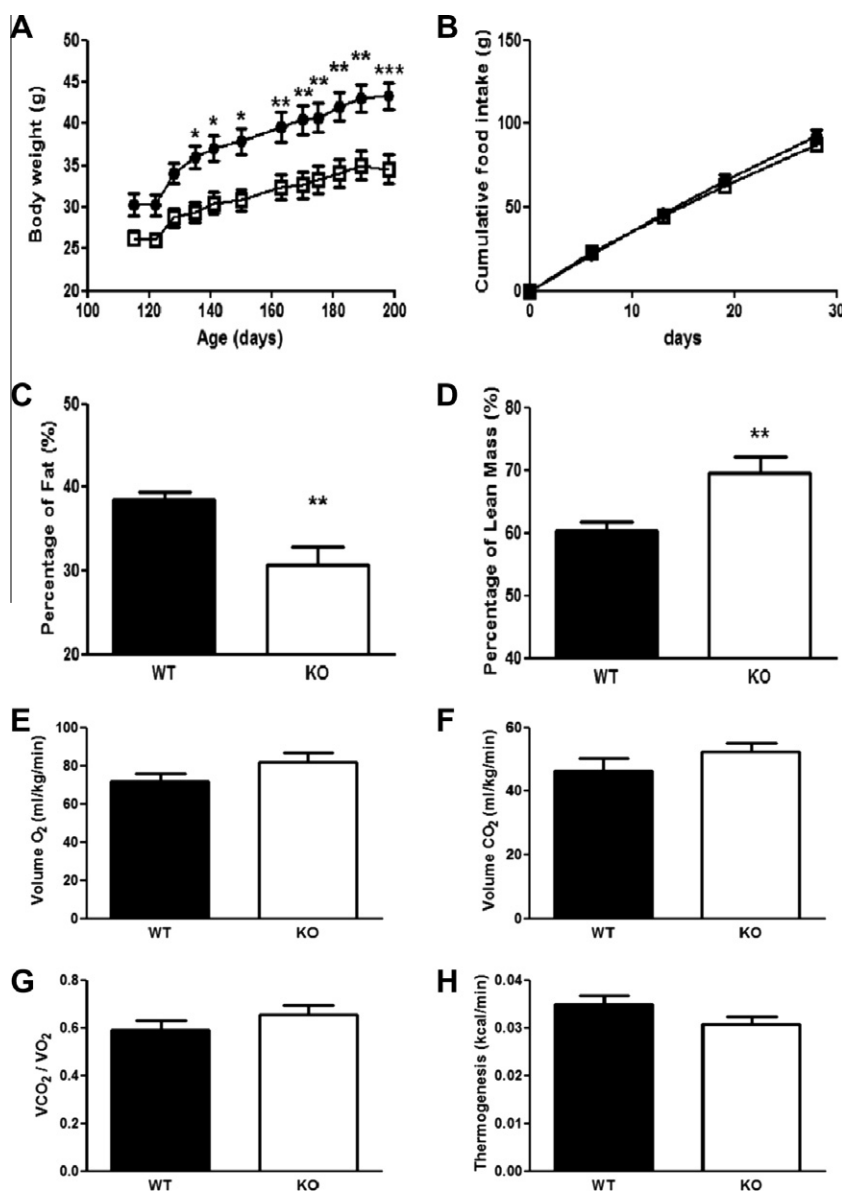


Fig. 1. Metabolic profile of GPR21 wildtype (closed symbols) and knockout (open symbols) mice were fed a 45% high fat diet for 12 weeks, starting at age 120 days. Body weight (A) and food intake (B) was measured weekly. The percentage of fat (C) and lean mass (D) were measured using a DEXA scanner. (E) Oxygen consumption (volume O₂ (ml/kg/min)) (F), carbon dioxide production (volume CO₂ (ml/kg/min)) (G), respiratory exchange ratio (VO₂/VCO₂) (C) and heat (kcal/min) (H) values were measured in GPR21 wildtype (closed bars) and knockout (open bars) mice. **p* < 0.05, ***p* < 0.01, ****p* < 0.001.

metabolic studies, mice were fed a 45% fat diet D12451i (Research Diet). Males were singly-housed during the studies to prevent potential cage mate fighting, while females were group-housed.

Mice were also weighed weekly. Food intake was measured by weighing the food pellets at the beginning and end of this one week period and calculating the difference.

2.2. Glucose tolerance test

Baseline glucose was measured in all animals using a drop of blood from a tail snip wound and Accu-chek active glucometers and test strips (Roche Diagnostics) (See Baribault, 2010 for protocol.) Then, 1 mg/kg glucose was injected intraperitoneally (i.p.) and glucose was measured again at 15, 30, 60 and 90 min after glucose administration.

2.3. Insulin tolerance test

Glucose was measured as described above. Then 1.5 U/kg of human insulin: Novolin R, 100 (NovoNordisk) was injected intraperitoneally to all mice. Glucose was measured again at 15, 30, 60, 90 and 120 min after insulin administration.

2.4. Total activity

To measure total activity, group-housed animals were taken from the animal colony room, weighed and numbered, and placed individually into a new cage with bedding. Two hours prior to the start of the dark cycle, the cage was placed in a 4 × 8 photo-beam frame connected to a computer for activity monitoring (Home Cage Photo-Beam Activity System, San Diego Instruments, San Diego, CA). Total photo-beam breaks were measured and recorded every 30 min for a total of 66 h. The number of photo-beam breaks was correlated with total activity.

2.5. Respiratory exchange rate

Mice were weighed and housed individually in a four-chamber Oxymax Equal Flow apparatus (Columbus Instruments) with access to food and water ad libitum. Mice were allowed to acclimate to the new environment for the first 24 h, after which the oxygen consumption (Volume O₂ (ml/kg/min)), carbon dioxide production (Volume CO₂ (ml/kg/min)), respiratory exchange ratio (VO₂/VCO₂) and heat (kcal/min) values were collected.

2.6. Multi-analyte profiling

At termination of the experiment, mice were euthanized and the blood was collected by cardiac puncture. Serum was separated and sent to Rules-based medicine for multi-analyte profiling (MAP).

2.7. Expression analysis

Total RNA from various tissues were obtained from Clontech, Biochain and Stratagene. Traces of genomic DNA were removed with DNase (Promega M6101), followed by purification with the RNeasy micro system (Qiagen Catalog: 74004). Quantitative real-time PCR was performed on a MX3000P Stratagene machine; all the PCR reagents were obtained from Stratagene; brilliant QRT-PCR; one-step (Catalog: 600551) and used following the manufacturer's instructions. All samples were analyzed in duplicate at least and corrected for mouse GAPDH (BC083149) run as an internal standard. Mouse GPR21 (NM_177383) gene sequences for probe and primers were as follows: (Probe: 5'-TTCAACATCTTCCGCATCTGCCAGC-3'; Primer

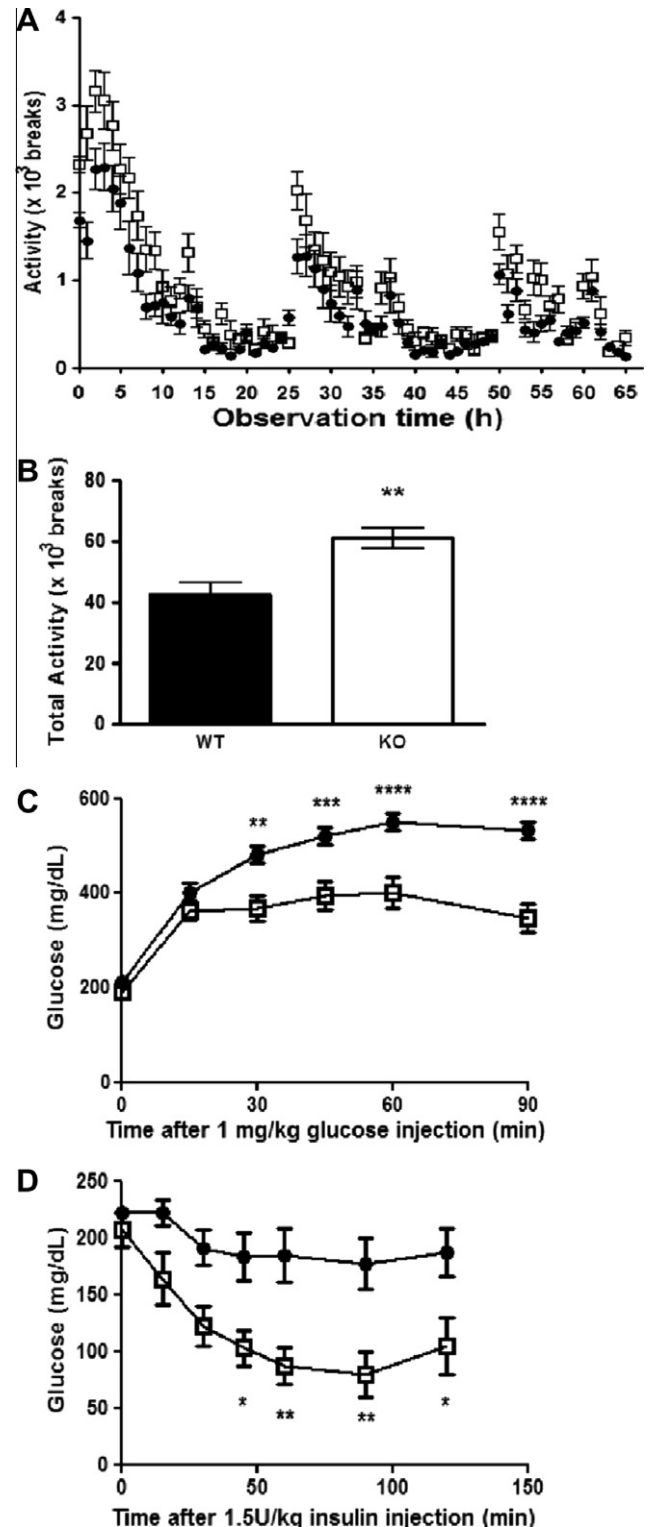


Fig. 2. (A) Locomotor activity of GPR21 wildtype (closed circles) and knockout (open squares) was measured with photobeam chambers. Number of beam breaks for each one hour interval over a three days period. (B) Total number of beam breaks over the same three days period. (C) Glucose tolerance test. After 12 weeks of DIO, 1 mg/kg glucose was administered i.p. Blood glucose levels were measured at 15, 30, 60, 90 and 120 min after glucose injection. (D) Insulin tolerance test. One week later, 1.5 IU/kg insulin was administered i.p. to the animals and glucose was measured at 15, 30, 60, 90 and 120 min after insulin injection. **p* < 0.05, ***p* < 0.01, ****p* < 0.001, *****p* < 0.0001.

forward: 5'-CCCTCATTGTCTGCTTCACGTA-3'; Primer reverse: 5'-CCTTCGCTGATTCTTTGTGT-3'.

2.8. Dual Energy X-ray Absorptiometry (DEXA) scanning

Mice were anesthetized by intraperitoneal injection of tribromoethanol (250 mg/kg) in PBS and then placed in a prone position on the platform of the PIXImus™ Densitometer (Lunar Inc.) for a DEXA scan. Using a Lunar PIXImus software, the bone mineral density (BMD), fat composition (%fat), lean mass and total tissue mass (TTM) were determined.

3. Results

3.1. GPR21 knockout mice are resistant to diet-induced obesity

GPR21 knockout mice looked healthy and showed no signs of disease when observed in their home cage environment. Heterozygous mating resulted in a normal mendelian transmission of the GPR21 knockout mutation.

When fed with a 45% (w/v) high fat diet, GPR21 knockout mice gained less weight than their wildtype littermates (Fig. 1A). Food intake was similar in both genotypes (Fig. 1B). After 12 weeks of treatment, knockout mice were leaner than wildtype controls as shown by the percentage of fat (Fig. 1C) and lean mass (Fig. 1D) measured by DEXA scanning.

To identify what mechanisms affect their energy balance, the respiratory exchange rate of the GPR21 knockout and control mice was measured over a 72 h period. We found no significant difference in the volume of oxygen consumption (Fig. 1E), volume of CO₂ release (Fig. 1F), in the ratio of those two values (Fig. 1G), or in the rate of heat generated (Fig. 1H).

The activity of GPR21 knockout and control mice was assessed using a photobeam chamber (Fig. 2A and B). Knockout mice were more active over a three days period, which may account for some of the difference observed in the energy balance.

3.2. GPR21 knockout mice show improved glucose tolerance and increased insulin sensitivity

After 12 weeks on a high fat diet, mice were fasted for four hours, and were injected intraperitoneally with 1 mg/kg glucose.

Although baseline glucose was not significantly different between the knockout and wildtype mice, mutant mice showed a higher ability to metabolize glucose (Fig. 2C). Consistently with those findings, when GPR21 knockout mice were injected with 1.5 IU/kg insulin, the glucose serum values were significantly reduced, indicating a higher sensitivity to insulin (Fig. 2D).

3.3. Inflammatory markers are reduced in GPR21 knockout mice

Insulin resistance is often associated with the presence of inflammatory markers. To test whether this was affected in the case in GPR21 knockout mice, we collected terminal blood samples and performed a multi-analyte profile of inflammatory markers. We observed a reduction in the chemokines: eotaxin, GCP-2, IP-10, lymphotactin, MCP-1, MCP-3, MIP-1 γ and MIP-3 β and in the C reactive and serum amyloid P proteins (Fig. 3). In contrast, no difference was seen in the levels of metabolic serum markers insulin and leptin.

3.4. GPR21 is a widely expressed gene

To gain some potential insights into the mechanisms of the GPR21 phenotype, we measured the expression of GPR21 in several organs. GPR21 is widely expressed in various organs involved in the regulation of energy balance such as brain, adipose tissue and liver, but also at high levels in the spleen (Fig. 4).

4. Discussion

GPR21 is an orphan G-protein-coupled receptor of previously unknown function that was first identified on the basis of its homology to other known GPCRs [4]. Here we report that GPR21 is involved in regulating body weight and glucose metabolism. GPR21 deficiency does not seem to affect food intake or the respiratory exchange rate. However, knockout animals are leaner, more active and have lower levels of chemokines: eotaxin, GCP-2, IP-10, lymphotactin, MCP-1, MCP-3, MIP-1 γ and MIP-3 β , and other serum inflammatory markers such as SAP and CRP. Interestingly, at the time of writing this manuscript, we became aware of another

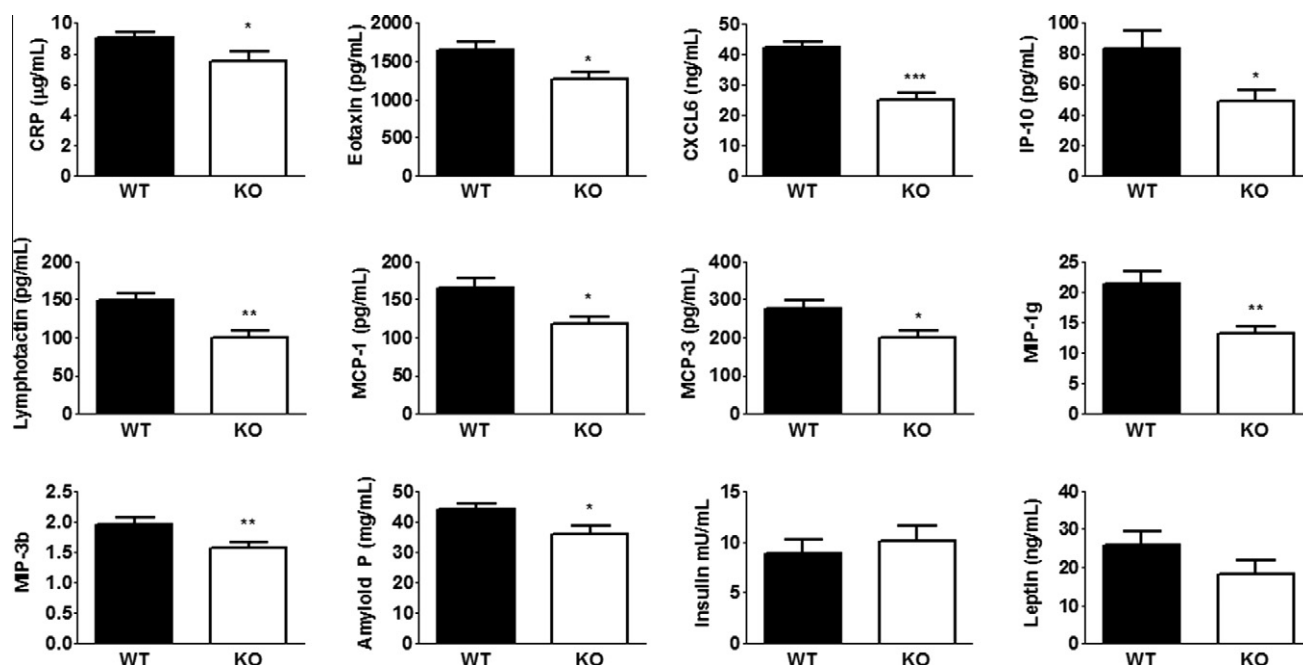


Fig. 3. Levels of inflammatory markers, CRP, Eotaxin, CXCL6, IP-10, Lymphotactin, MCP-1, MCP-3, MIP-1 γ , MIP-3 β , Amyloid P, and of the metabolic markers insulin and leptin in GPR21 wildtype (closed) and knockout (open) mice. * $p < 0.05$, ** $p < 0.01$.

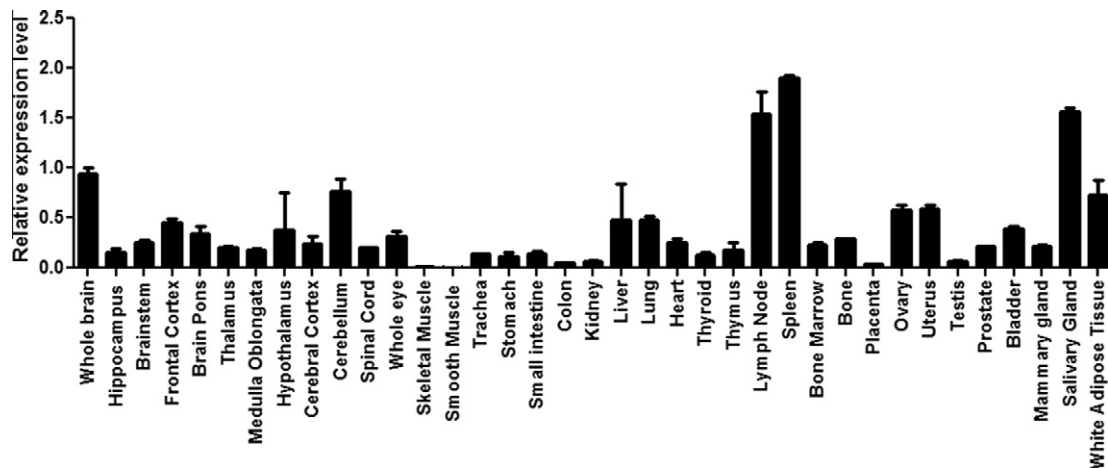


Fig. 4. Expression of GPR21 in various tissues as measured by Q-PCR.

group who had obtained similar results with the GPR21 KO mice (Drs. Osborn and Olefsky, Dept. Medicine, University of California–San Diego, La Jolla, CA, USA, personal communication), including a reduction of the chemokine MCP-1, the ligand for CCR2, in adipose tissues. This is of particular interest because of the recent emphasis on the role of a chronic low grade inflammation as a significant contributor to insulin resistance during the progression to type 2 diabetes mellitus.

Serum CRP and serum amyloid protein (SAP) are reduced in GPR21 knockout mice. They are members of the pentraxin family. They are produced by hepatocytes and are involved in autoimmunity and in acute-phase inflammatory responses [8]. Numerous studies have shown that elevated values of such molecules are associated with a higher risk to develop obesity and diabetes [9,10].

GPR21 is a broadly expressed gene and consequently the mechanism by which GPR21 exerts its metabolic phenotype is difficult to pinpoint. GPR21 is found widespread throughout several brain regions, and is expressed in liver, adipose tissues and the spleen. Another potential mechanism for the action of GPR21 could be centrally-mediated causing an increase in ambulatory activity.

GPR21 is still an orphan GPCR. The identification of the GPR21 ligand will be a key element to the elucidation of its mechanism. Looking at the closest relatives of GPR21 in the phylogenetic tree of the GPCR family reveals little about the putative nature of GPR21 ligand, i.e., a small molecule or a peptide [11]. Its closest relative is GPR52 with 71% identity, yet GPR52 is also an orphan GPCR [5].

Altogether, the current findings show that the deletion of GPR21 improves insulin sensitivity in a diet-induced model of obesity and that the signaling of this GPCR may be a new therapeutic target in the treatment of obesity and diabetes.

Acknowledgments

We thank Deltagen for providing the mutant animals and the personnel of the Research Animal Facility (Amgen, San Francisco) for care and monitoring of animals.

References

- [1] W.K. Kroeze, D.J. Sheffler, B.L. Roth, G-protein-coupled receptors at a glance, *J. Cell Sci.* 116 (2003) 4867–4869.
- [2] R.J. Lefkowitz, Historical review: a brief history and personal retrospective of seven-transmembrane receptors, *Trends Pharmacol. Sci.* 25 (2004) 413–422.
- [3] K.L. Pierce, R.T. Premont, R.J. Lefkowitz, Seven-transmembrane receptors, *Nat. Rev. Mol. Cell Biol.* 3 (2002) 639–650.
- [4] B.F. O'Dowd, T. Nguyen, B.P. Jung, A. Marchese, R. Cheng, H.H. Heng, L.F. Kolakowski Jr., K.R. Lynch, S.R. George, Cloning and chromosomal mapping of four putative novel human G-protein-coupled receptor genes, *Gene* 187 (1997) 75–81.
- [5] M. Sawzdargo, T. Nguyen, D.K. Lee, K.R. Lynch, R. Cheng, H.H. Heng, S.R. George, B.F. O'Dowd, Identification and cloning of three novel human G protein-coupled receptor genes GPR52, PsiGPR53 and GPR55: GPR55 is extensively expressed in human brain, *Brain Res. Mol. Brain Res.* 64 (1999) 193–198.
- [6] S.H. Xiao, J.D. Reagan, P.H. Lee, A. Fu, R. Schwandner, X. Zhao, J. Knop, H. Beckmann, S.W. Young, High throughput screening for orphan and liganded GPCRs, *Comb. Chem. High Throughput Screen* 11 (2008) 195–215.
- [7] J.N. Bresnick, H.A. Skynner, K.L. Chapman, A.D. Jack, E. Zamiara, P. Negulescu, K. Beaumont, S. Patel, G. McAllister, Identification of signal transduction pathways used by orphan G protein-coupled receptors, *Assay Drug Dev. Technol.* 1 (2003) 239–249.
- [8] M.S. Kravitz, M. Pitashny, Y. Shoenfeld, Protective molecules—C-reactive protein (CRP), serum amyloid P (SAP), pentraxin3 (PTX3), mannose-binding lectin (MBL), and apolipoprotein A1 (Apo A1), and their autoantibodies: prevalence and clinical significance in autoimmunity, *J. Clin. Immunol.* 25 (2005) 582–591.
- [9] P. Arora, B. Garcia-Bailo, Z. Dastani, D. Brenner, A. Villegas, S. Malik, T.D. Spector, B. Richards, A. El-Sohehy, M. Karmali, A. Badawi, Genetic polymorphisms of innate immunity-related inflammatory pathways and their association with factors related to type 2 diabetes, *BMC Med. Genet.* 12 (2011) 95.
- [10] Z. Su, Y. Li, J.C. James, A.H. Matsumoto, G.A. Helm, A.J. Lusis, W. Shi, Genetic linkage of hyperglycemia, body weight and serum amyloid-P in an intercross between C57BL/6 and C3H apolipoprotein E-deficient mice, *Hum. Mol. Genet.* 15 (2006) 1650–1658.
- [11] D.K. Vassiliatis, J.G. Hohmann, H. Zeng, F. Li, J.E. Ranchalis, M.T. Mortrud, A. Brown, S.S. Rodriguez, J.R. Weller, A.C. Wright, J.E. Bergmann, G.A. Gaitanaris, The G protein-coupled receptor repertoires of human and mouse, *Proc. Natl. Acad. Sci. USA* 100 (2003) 4903–4908.